

Polyurethane scaffold with in situ swelling capacity for nucleus pulposus replacement

LI, Zhen, LANG, Gernot, CHEN, Xu, SACKS, Hagit, MANTZUR, Carmit, TROPP, Udi, MADER, Kerstin T. <<http://orcid.org/0000-0002-2524-6512>>, SMALLWOOD, Thomas C., SAMMON, Chris <<http://orcid.org/0000-0003-1714-1726>>, RICHARDS, R. Geoff, ALINI, Mauro and GRAD, Sibylle

Available from Sheffield Hallam University Research Archive (SHURA) at:

<http://shura.shu.ac.uk/12665/>

This document is the author deposited version. You are advised to consult the publisher's version if you wish to cite from it.

Published version

LI, Zhen, LANG, Gernot, CHEN, Xu, SACKS, Hagit, MANTZUR, Carmit, TROPP, Udi, MADER, Kerstin T., SMALLWOOD, Thomas C., SAMMON, Chris, RICHARDS, R. Geoff, ALINI, Mauro and GRAD, Sibylle (2016). Polyurethane scaffold with in situ swelling capacity for nucleus pulposus replacement. *Biomaterials*, 84, 196 - 209.

Copyright and re-use policy

See <http://shura.shu.ac.uk/information.html>

Polyurethane scaffold with *in situ* swelling capacity for nucleus pulposus replacement

Zhen Li^{1†}, Gernot Lang^{1,4†}, Xu Chen¹, Hagit Sacks², Carmit Mantzur², Udi Tropp², Kerstin T Mader³, Thomas C Smallwood³, Chris Sammon³, R Geoff Richards^{1,4}, Mauro Alini¹, Sibylle Grad^{1*}

¹AO Research Institute Davos, Davos, Switzerland;

²Nicast Ltd., Lod, Israel;

³Sheffield Hallam University, Sheffield, United Kingdom

⁴Department of Orthopedic and Trauma Surgery, Freiburg University Medical Center, Freiburg, Germany

Running title:

Polyurethane scaffold with *in situ* swelling capacity for nucleus pulposus replacement

[†]these authors contributed equally to the manuscript

*Address for correspondence:

Sibylle Grad, PhD
AO Research Institute Davos
Clavadelerstrasse 8
7270 Davos
Switzerland
Tel: +41 81 414 2480
Fax: +41 81 414 2288
Email: sibylle.grad@aofoundation.org

Abstract

Nucleus pulposus (NP) replacement offers a minimally invasive alternative to spinal fusion or total disc replacement for the treatment of intervertebral disc (IVD) degeneration. This study aimed to develop a cytocompatible NP replacement material, which is feasible for non-invasive delivery and tunable design, and allows immediate mechanical restoration of the IVD. A bi-phasic polyurethane scaffold was fabricated consisting of a core material with rapid swelling property and a flexible electrospun envelope. The scaffold was assessed in a bovine whole IVD organ culture model under dynamic load for 14 days. Nucleotomy was achieved by incision through the endplate without damaging the annulus fibrosus. After implantation of the scaffold and *in situ* swelling, the dynamic compressive stiffness and disc height were restored immediately. The scaffold also showed favorable cytocompatibility for native disc cells. Implantation of the scaffold in a partially nucleotomized IVD down-regulated catabolic gene expression, increased proteoglycan and type II collagen intensity and decreased type I collagen intensity in remaining NP tissue, indicating potential to retard degeneration and preserve the IVD cell phenotype. The scaffold can be delivered in a minimally invasive manner, and the geometry of the scaffold post-hydration is tunable by adjusting the core material, which allows individualized design.

Keywords

Biphasic polyurethane scaffold; *in situ* swelling; nucleus pulposus replacement; organ culture; nucleotomy; intervertebral disc degeneration

Introduction

The intervertebral disc (IVD) is a complex tissue structure with important mechanical functions. It consists of a central part, the nucleus pulposus (NP), the surrounding annulus fibrosus (AF), and the cartilaginous endplates which provide the permeable connections to the bony vertebrae. The main function of the NP is to absorb and distribute mechanical load exerted on the spinal column. To fulfil this function, the NP contains specific extracellular matrix components rich in proteoglycans that allow the maintenance of a highly hydrated state and high swelling pressure [1].

IVD degeneration is associated with changes in extracellular matrix composition that often have biomechanical consequences and can lead to painful and debilitating conditions. The resulting neck and low back pain are major determinants of discomfort and disability and are the origin of enormous socio-economic health care problems worldwide [2-4]. Treatment methods range from physical therapies and pain relieving medication to highly invasive surgical procedures. Discectomy is often performed in cases of disc bulging or herniation to relieve the painful pressure on neural elements. Spinal fusion is another standard treatment intended to relieve pain by reducing motion across the joint. However, removal of disc tissue and fusion alter the biomechanical function and can accelerate IVD degeneration at adjacent levels [5]. Due to the limited healing potential and harsh nutritional conditions of adult IVDs, loss or failure of the extracellular matrix is virtually irreversible and requires restoration. Implants for total IVD replacement have been developed in order to preserve the motion at the operated level. However, the procedure is highly invasive and may not be appropriate at early stages of degeneration; in addition the long term effects are still uncertain [6].

Functionally, during IVD degeneration the NP becomes dehydrated, is replaced by fibrous tissue, and loses its high osmotic pressure [2, 7, 8]. The severe loss of water content in the NP also causes a reduction in disc height. NP replacement therapy has therefore been proposed as a less invasive alternative method to spinal fusion or total IVD replacement [9]. An ideal NP replacement material would allow immediate redistribution of loads and restoration of disc height, while maintaining the flexibility of the spine. Various synthetic polymeric materials have been described as potential NP substitutes that may be delivered as injectable hydrogel or pre-formed material [10-13]. However, several concerns still exist in their application. While conventional injectable hydrogels can be delivered through the AF in a minimally-invasive manner, their generally weak mechanical properties do not allow direct restoration of the disc height and mechanical function; in addition, their three-dimensional structure is difficult to control and there is a substantial risk of material leakage with adverse effects. Pre-formed polymers and scaffolds have the advantage of improved structural control and faster response to external mechanical forces. Nevertheless, their application requires a more invasive procedure, and unwanted outcomes such as material displacement may occur [14-16].

The polyurethane (PU) family of biomaterials has been introduced for medical use because of their elastomeric properties. By varying the composition of the monomer units and the size of the blocks of the dissimilar monomers within the polymer chain, these properties can be tailored. As such, PU has been used in applications in which an elastomeric material is likely to enhance the success or longevity of the implant. Specifically, PU has been used in cardiovascular applications, where material flexibility is important, such as for catheters, insulations, vascular prostheses, heart valves or assist devices [17]. Furthermore, a range of tissue replacement or augmentation materials are based on PU, especially as wound dressing for skin

regeneration [18]. Among the PU family, polycarbonate urethanes have demonstrated improved biostability and are therefore preferred for many applications [19, 20]. The function of the intervertebral disc relies on the elastomeric nature of the matrix components and fluid of which they are constituted; hence, PU is an attractive material for IVD restoration. In fact PU based materials have been used in spinal surgery and the overall mechanical and biological properties indicate no long-term problems to date; though information on their application as pure NP replacement is scarce [21].

Taking into account the requirements for an NP substitute, we have developed a new bi-phasic polyurethane (PU) scaffold consisting of a highly hydrophilic core material with significant instant swelling capabilities and an electrospun envelope. The functions of the envelope are to assure the structural control of the implant after swelling *in situ* and to facilitate cell attachment and tissue integration to keep the implant stable also under mechanical load. Moreover, the unique flat geometry and flexible shape of the bi-phasic scaffold system allow minimally invasive administration into the NP of the IVD.

The aim of this work was to assess the mechanical, swelling properties and the cytocompatibility of the scaffold materials. A whole IVD organ culture model was then used to test the hypothesis that the implanted scaffold could restore the disc height and mechanical stiffness in a nucleotomized IVD. Histological and gene expression analyses were performed to evaluate the biological response of the disc cells and tissues to the implanted scaffold.

Materials and Methods

1. Fabrication and characterization of PU scaffolds

1.1. Fabrication of PU scaffolds

PU scaffolds with swelling capability were manufactured to obtain implants with a flat discoid structure. The scaffolds are composed of a core film which swells to a hydrogel following contact with an aqueous medium, and an envelope composed of electrospun polymer mixture with a fibrous mat structure (Fig. 1 A). The core solution was prepared with the ether-based hydrophilic urethane HydroMed™ (HM, AdvanSource Biomaterials), which was dissolved at a concentration of 20 % (w/w) in 95% ethanol (Bio-Lab) by stirring overnight at room temperature. A predetermined solution volume was casted on a flat glass plate, dried for three days to ensure solvent residues evaporation and then cut into discs at a diameter of 3, 5 and 8 mm for manufacturing scaffold at external diameter of 6, 8 or 9, and 14 mm, respectively.

For production of the envelope a mixture was prepared by combining the polycarbonate urethanes Chronoflex™ (CF, AdvanSource Biomaterials) and HM. In order to select the optimal ratio of CF to HM in the envelope formulation, several ratios were tested. Wetting time was visually inspected until color change observed and mechanical property was evaluated by measurement of the tensile strength. As shown in Table 1, addition of HM to CF resulted in decrease in the mechanical strength and reduced the wetting time. Optimal balance between wetting, mechanical strength and manufacturing considerations by electrospinning resulted in the selection of CF:HM w/w ratio at 10:1. The polyurethane mixture was then dissolved at a concentration of 13% (w/w) in a solvent mixture of 1:2 w/w N-N-dimethylformamide (BioLab) and dioxane (BioLab). Electrospun envelope structures at a thickness of 200 µm were fabricated according to specifications for strong fibers at a range of 0.5-

2 μm and porosity of $\sim 70\%$. The following electrospinning parameters were applied at an environment of 40% relative humidity and 28°C . A collector at diameter of 50 mm and length of 150 mm with rotating speed (ω) of 120 rpm was used. A five needles spinneret was used (22 G, 25 mm length) at linear speed of 57 mm/sec and traverse shuttle of 170 mm. The spinneret was placed 260 mm from the collector. A potential of 60 kV, solution flow rate of 14 mL/h and consumption of 10 mL were applied.

Following electrospinning the envelope sheet was dried overnight at room temperature and then at $50 \pm 5^\circ\text{C}$ for 48 hours. The dried envelope sheets were cut into discs of 20 mm diameter before scaffold assembly.

Core discs at predetermined content (see 1.3) and size were wrapped by two envelope discs that were heat sealed using custom made tools (Fig. 1 B). The sealing conditions were 4 seconds at pressure of 3 bar and temperature of 118°C . The PU scaffold was then cut into its final size, at a diameter of 6, 8, 9 or 14 mm. The scaffolds were sterilized in a cold-cycle (37°C) ethylene oxide process and subsequently evacuated at room temperature and 150 mbar for 7 days.

A delivery system for non-invasive injection of the PU scaffolds was developed by Melab Medizintechnik und Labor GmbH (Germany). The PU scaffolds at diameters of 6-14 mm can be rolled into a tube of 2.8-5 mm diameter and delivered through a needle with insertion guide. A demonstration of the delivery process is shown in Figure 1 C.

1.2. Structure characterization of the PU scaffold envelope

The electrospun envelope sheet material was examined using scanning electron microscopy (SEM). Electron micrographs were recorded for both sides and cross sectional areas of the electrospun envelope. Samples were snap-frozen in liquid

nitrogen and fractured into 2 or more pieces to obtain a cross-sectional edge. Samples were then mounted onto metallic stubs and coated with gold (~1 nm; Q150T-ES sputter coater, Quorum, UK) and their morphology observed on a Nova Nano SEM (FEI, Netherlands; Everhart-Thornley Detector in field-free lens mode) at 2,000x and 10,000x magnifications. Fiber dimensions were measured in Q-capture pro (QImaging, Canada) using the scale bar of the SEM micrograph as a reference for each image. Measurements were taken from three samples. Approximately 50 fibers were randomly selected for each micrograph.

1.3. Swelling capacity and kinetics of PU scaffolds

PU scaffolds with a diameter of 14 mm containing various dry weights of core (14 to 97 mg, n=18) were incubated in aqueous medium at room temperature for 24 hours. The swelling capacity was calculated by measurement of the scaffold dry weight before swelling and the scaffold wet weight after incubation. Results were expressed as % swelling of core and/or % weight gain of PU scaffold. Swelling capacities of PU scaffolds with diameter of 6, 8, 9, and 14 mm were also measured at fixed core content (3.4 mg and 4.5 mg for 6 mm PU scaffold, 12 mg for 8 mm and 9 mm PU scaffold, 40 mg for 14 mm PU scaffold). Swelling kinetics measurements were carried out with scaffolds with diameter of 6 and 14 mm using various core contents (3.4 mg, 4.5 mg and 6.3 mg for 6 mm PU scaffold, 30 mg, 40 mg and 60 mg for 14 mm PU scaffolds) in order to determine the time to reach significant swelling.

1.4. Cytocompatibility of PU scaffolds

To assess the potential release of cytotoxic components that might have remained or developed from the scaffold production process or the sterilization method, core and

envelope discs were incubated in Dulbecco's Modified Eagle Medium (DMEM, with 4.5 g/L glucose, Gibco, Paisley, UK) containing 100 U/mL penicillin and 100 µg/mL streptomycin (1% Pen/Strep) (all products from Gibco) at 37°C under normoxic condition. The conditioned medium was collected after 3, 5 and 7 days. Nucleus pulposus cells (NPCs) were isolated from 4-10 months old bovine caudal IVD and cultured with DMEM, 1% Pen/Strep, 10% fetal calf serum (FCS, Gibco) at 37°C under normoxic condition [22]. Human bone marrow aspirates were obtained with ethical approval from the Swiss cantonal authorities (KEK 188/10) and informed consent. Bone marrow derived mesenchymal stem cells (MSCs) were isolated by Ficoll cushion and expanded with alpha modification of Eagle's medium (aMEM, Gibco), 1% Pen/Strep, 10% FCS, 5 ng/mL recombinant human basic fibroblast growth factor (Fitzgerald, Acton, USA) at 37°C under normoxic condition [23]. Passage 1 NPCs and passage 2 MSCs were seeded into 96-well plates and cultured in DMEM with 1% Pen/Strep, 2.5% FCS and 50% conditioned medium of PU core and envelope for 24 hours or 72 hours at 37°C under normoxic condition. Cell viability was determined with WST-1 cell proliferation reagent (Roche, Mannheim, Germany) according to an established protocol [24]. Cell viability of the samples was normalized to the positive control cells cultured in DMEM with 1% Pen/Strep and 2.5% FCS.

A cell attachment study was performed to examine the capacity of the envelope to support cell attachment and growth. Passage 1 bovine NPCs were seeded on the top side of the envelope at a cell density of 100,000 cells per envelope (diameter 14 mm). Cell-envelope constructs were cultured in DMEM with 1% Pen/Strep and 10% FCS for 7 days at 37°C under normoxic condition. After 1 and 7 days of culture, samples were digested with 0.5 mg/mL proteinase-K (2.5 U/mg, Roche, Mannheim, Germany) at 56°C overnight. DNA content was measured spectrofluorometrically using the

Picogreen assay (Invitrogen, Carlsbad, USA) to evaluate the cell proliferation. Samples were also prepared for SEM imaging of the top surfaces and cross-sections of the envelopes to evaluate the cell morphology and attachment on the material surface. Cell-seeded envelopes were fixed in 2.5% glutaraldehyde in 0.1 M PIPES buffer, and dehydrated in a series of graded concentrations of ethanol before critical point drying (Quorum Technologies Ltd, East Sussex, UK). Thereafter, samples were mounted on metallic stubs with silver paint, sputter coated with gold/palladium (10 nm) and imaged by SEM (Hitachi S-4700, Tokyo, Japan).

2. IVD organ culture – IVD dissection, nucleotomy, PU scaffold implantation, and dynamic loading

For assessment of the PU scaffold in organ culture which supplies a microenvironment close to the *in vivo* situation, bovine caudal spines (4-10 months) were obtained from local abattoirs and harvested aseptically within three hours after death. After removal of the soft tissue, IVDs were dissected by means of a band saw (model 30/833, Exakt Apparatebau, Norderstedt, Germany) proximal and distal to the cartilaginous endplates, and the endplates of each IVD were cleaned with a Pulsavac jet-lavage system (Zimmer, IN, USA) [22]. Initial disc height and diameter were recorded before IVDs were washed with PBS (pH 7.4) containing 10% Pen/Strep for 15 min. Then IVDs were transferred to a six-well plate containing IVD culture medium and incubated overnight at 37°C, 85% humidity and 5% CO₂. The IVD culture medium was composed of DMEM with 4.5 g/L glucose supplied with 2% FCS, 1% Pen/Strep, 1% ITS+ Premix (Discovery Labware, Inc., Bedford, USA), 50 µg/mL ascorbate-2-phosphate (Sigma-Aldrich, St. Louis, USA) and 0.1% Primocin. After dissection, the disc height of the bovine IVDs used for the current study ranged from

7 to 14 mm and the disc diameter ranged from 13 to 20 mm. IVDs from each tail were randomly assigned among experimental groups to obtain similar average disc size and distribution of disc levels for each group.

A partial nucleotomy model [22] was used to mimic the clinical case of a large NP defect with relatively healthy non-degenerated surrounding disc tissue. To reach a nucleotomy fraction of approximately 50% of the total NP volume for different sizes of IVDs, a NP cavity with diameter of 4 mm was created in small IVDs with diameter of 13-16.5 mm; in IVDs with diameter of 16.5-20 mm, a NP cavity with diameter of 6 mm was created. IVDs were nucleotomized through the endplate by central incisions with a biopsy punch of 4 or 6 mm diameter and a number 11 blade. After removing an endplate core, the NP tissue below the endplate core reaching until the distal endplate was excised. IVDs and endplate stoppers were preserved in gauze moistened with IVD culture media. Pilot experiments had revealed that dry PU scaffolds with 6 mm or 9 mm diameter obtained a diameter of 4 mm or 6 mm after hydration. Therefore, dry PU scaffolds with 6 mm or 9 mm diameter were implanted into the NP defects with 4 mm or 6 mm diameter, respectively. The PU scaffolds with a flat discoid structure were delivered into the NP cavity with forceps, and positioned parallel to the endplate of the IVD. After implantation of the dry PU scaffold, the removed endplate stopper was immediately re-inserted, and the crack between the stopper and the remaining endplate was sealed by polymethyl methacrylate (PMMA, Vertecem Mixing Kit, Synthes, Teknimed S.A., Bigorre, France) according to manufacturer's instruction. For each IVD, approximately 100–150 mg of PMMA was applied.

A bioreactor system was used to mimic physiologically relevant loading conditions of cultured IVDs [25]. IVDs were placed in custom-made chambers filled with 2 mL IVD

1
2
3
4
5
6
7
8
9
10
11
12
13
14
15
16
17
18
19
20
21
22
23
24
25
26
27
28
29
30
31
32
33
34
35
36
37
38
39
40
41
42
43
44
45
46
47
48
49
50
51
52
53
54
55
56
57
58
59
60
61
62
63
64
65

276 culture medium, and loaded dynamically for 3 hours/day at 0-0.1 MPa, 0.1 Hz. After
277 dynamic loading IVDs were transferred to 6-well plates with 5 mL IVD culture medium
278 for free swelling recovery overnight. It has been reported that the diurnal disc height
279 loss of human lower lumbar discs was 11.1% [26]. Therefore, a 10% diurnal disc
280 height loss was considered as physiological for organ cultured discs. In our previous
281 study, this loading protocol applied on bovine caudal IVDs of similar age has shown
282 to be physiologically relevant, as indicated by disc height loss and recovery at
283 physiological level [27].

285 3. IVD organ culture - mechanical effect of PU scaffold implantation after 1 day of 286 loading

287 3.1. Experimental groups

288 To investigate the mechanical repair effect of the PU scaffold, dynamic load was
289 performed on partial nucleotomized IVDs implanted with PU scaffold (Scaffold group)
290 for 3 hours. Empty IVDs served as negative controls (Empty group). The experiments
291 were performed using IVDs from 6 bovine tails, with 2 IVDs from each tail randomly
292 assigned to one of the two experimental groups.

294 3.2. Dynamic compressive stiffness modulus

295 Dynamic compressive stiffness modulus was measured for each IVD at the following
296 time points: after dissection and overnight free swelling culture (intact), after partial
297 nucleotomy (defect), after refilling with the PU scaffold and free swelling culture
298 overnight (refilled), and after dynamic load and free swelling recovery. Measurement
299 was performed using a custom-made chamber and a Bose 3220 instrument (Bose,
300 MN, USA) as described previously [22]. IVDs were pre-loaded with 10% strain (based

on initial disc height after dissection) for 3 min, and then loaded with 10 cycles of sinusoidal compression at 5-15% of strain (based on initial disc height after dissection) at a frequency of 0.1 Hz for 100 seconds. Dynamic compressive stiffness modulus was calculated for each loading cycle as the stress segment divided by the strain segment (10%). Average value of 10 cycles was taken for each IVD at each time point. The stiffness modulus was then normalized to the value of respective intact IVD.

3.3. Disc height change

Disc height was measured with a caliper at the following time points: after dissection, after dissection and free swelling culture overnight (intact), after partial nucleotomy (defect), after refilling with biomaterial and free swelling culture overnight (refilled), after dynamic load, and after free swelling recovery. Each IVD was measured at four positions and the average value was used to calculate the percentage of disc height change. Disc height change was normalized to the initial dimension after dissection.

4. IVD organ culture – mechanical and biological effects of PU scaffold implantation after 14 days of loading

4.1. Experimental Groups

The biological repair effect of the PU scaffold was investigated after 14 days of dynamic load. Empty IVDs served as negative controls. The experiments were performed using bovine IVDs from 12 tails, with 2 IVDs from each tail randomly assigned to one of the two experiment groups.

4.2. Disc height change

The disc height was measured with a caliper at the following time points: day 0 after dissection, day 1 after 1st load, day 2 after 1st recovery, day 7 after 7th load, day 8 after 7th recovery, day 14 after 14th load and day 15 after 14th recovery. Each IVD was measured at four positions and the average value was used to calculate the percentage of disc height change. Disc height change was normalized to the initial dimension after dissection.

4.3. Biochemical and gene expression analysis

After free swelling recovery on day 15 cartilaginous endplates of each IVD were removed and remaining NP and AF tissues were harvested by using a biopsy punch and a scalpel blade. Approximately 100 mg of each AF and NP tissue was used for RNA extraction; 50 mg of each AF and NP tissue was digested within 0.5 mg/mL proteinase K at 56°C overnight for glycosaminoglycan (GAG), collagen and DNA content measurement; 30 mg of NP tissue was used for [³⁵S] sulfate incorporation assay to assess proteoglycan synthesis rate.

For RNA extraction, tissue samples were flash frozen and pulverized in liquid nitrogen and homogenized using a TissueLyser (Qiagen, Venlo, Netherlands). Total RNA was extracted with TRI Reagent (Molecular Research Center) and reverse transcription was performed with SuperScript VILO cDNA Synthesis Kit (Life Technologies, Carlsbad, CA). Quantitative real-time PCR was performed using the Step-One-Plus instrument (Life Technologies). The sequences of custom designed bovine primers and TaqMan™ probes are shown in Table 2. For amplification of 18S ribosomal RNA (18S, 4310893E), Versican (Bt03217632_m1), and Biglycan (BGN, Bt03244532_m1), gene expression assays from Applied Biosystems (Life

Technologies) were used. Comparative Ct method was performed for relative quantification of target mRNA with 18S ribosomal RNA as endogenous control.

The GAG content in the NP and AF tissues was determined by using the 1,9-dimethylmethylene blue dye (DMMB) method [28]. Quantification of the total amount of collagen in NP and AF samples was performed using the hydroxyproline assay as described earlier [29]. DNA content was measured spectrofluorometrically using Hoechst (33258) dye.

To determine the proteoglycan synthesis rate NP tissue was incubated for 16-20 hours in IVD culture media supplemented with 2.5 μCi ^{35}S -sulfate /mL ($\text{Na}_2^{35}\text{SO}_4$; PerkinElmer, Schwerzenbach, Switzerland). Thereafter NP tissue was digested with 0.5 mg/mL proteinase K at 56°C overnight. Conditioned medium and proteinase K digested tissue samples were processed with PD-10 desalting columns (GE Healthcare, Glattbrugg, Switzerland) and radioactive counts were measured by Wallac 1414 Liquid Scintillation Counter (PerkinElmer, Schwerzenbach, Switzerland). The counts per minute (cpm) were normalized to the DNA content of the respective samples.

4.4. Safranin O/Fast Green staining

After free swelling recovery on day 15, whole IVDs with implanted PU scaffolds were fixed in 70% methanol and transferred into PBS with 5% sucrose at 4°C overnight before cryosectioning. Transverse sections of IVDs were cut at a thickness of 12 μm . Sections were stained with 0.1% Safranin-O and 0.02% Fast Green to reveal proteoglycan and collagen deposition respectively, and counterstained with Weigert's Haematoxylin to reveal cell distribution.

4.5. Fourier transform infrared (FTIR) spectroscopic imaging

After free swelling recovery on day 15, a set of IVDs (n=1 per group) were decalcified and subsequently embedded in paraffin. Four micrometre sagittal IVD sections were cut and mounted on custom made reflective 316 stainless steel slides for infrared analysis. FTIR microscopic images were collected using an Agilent 680-IR FTIR spectrometer (ISys50®, Malvern Instruments Limited, Worcestershire, UK) coupled to a FTIR imaging microscope fitted with a liquid nitrogen cooled 64 x 64 mercury-cadmium-telluride focal plane array detector (FPA) and an automated sampling stage. For each sample, an area of 71 x 192 pixels (approximately 6.3 x 16.8 mm) was mapped in transfectance mode. Spectra were attained with a spectral resolution of 4 cm⁻¹ over a wavenumber range of 950-1900 cm⁻¹. Data was pre-processed by performing a second derivative (Savitsky-Golay ISys50 software, Filter order 3, filter length 15) on the spectra to reduce baseline effects and assist the resolution of weaker absorption peaks [30]. Pixels within the tissue section where spectra indicated only the presence of paraffin or the substrate were identified and masked using spectral statistics (ISys50, histogram). Regions of interest (ROI; 10 x 192 pixels) across the middle of each sagittal section were cut and compiled to one data matrix. The data set was analyzed using a multivariate curve resolution-alternating least squares algorithm (MCR-ALS) described by Andrew and Hancewicz [31] and Wang et.al. [32]. MCR-ALS was carried out using the MCR-ALS v1.6 software (MCRv1.6 Copyright © 2003-2004 Unilever) on two wavenumber regions of 950-1600 cm⁻¹ and 950-1300 cm⁻¹ with the following settings; initial estimates: 4 -10F, NIPALS, ALS; ALS constraints: MALS-2D, none, 1e-005, 500. General tissue, collagen type I, collagen type II and proteoglycan distributions were estimated according to previous studies that have shown good agreement between (immuno-) histological staining and the integrated peak area of the 2nd derivative of the amide III spectral region

(1186-1297 cm^{-1}) as well as MCR-ALS score maps [33]. Additionally, average matrix component per tissue distribution across ROIs were calculated and are represented as estimated component per tissue distribution line profiles across the normalized width (0-100%) of each IVD.

5. Statistical analysis

SPSS 21.0 statistical software was used for statistical analysis. One sample Kolmogorov–Smirnov test was used to define whether the data were normally distributed (normal distribution at $p > 0.1$). For data that were normally distributed, unpaired T test was used to determine differences between Empty and Scaffold groups. For data that were not normally distributed, Mann-Whitney U was used to determine differences between Empty and Scaffold groups. A p-value < 0.05 was considered statistically significant.

Results

1. Characterization of PU scaffold

1.1. Structure characterization of PU scaffold envelope

Randomly arranged, homogenous fibers could be observed in the SEM micrographs of electrospun PU scaffold envelopes, indicating a successful mixing and electrospinning of the Chronoflex and Hydromed mixture (Fig. 2). The generated fibers had an average thickness of $0.84 \pm 0.52 \mu\text{m}$.

1.2. Swelling capacity and kinetics of PU scaffolds

Swelling capacity of the scaffold (14 mm diameter) at various core contents is shown in Fig. 3. At the core content range tested, the swelling ratio of the scaffold increased

with the increase in core content. Swelling capacity of the different scaffold sizes and core amounts is summarized in Table 3. At the range tested, the core material reached similar swelling percentage (~800%) regardless of scaffold size. The scaffold weight gain increased with the increase in size.

Swelling kinetics is shown in Fig. 4. The swelling rate was relatively fast after immersion in aqueous medium. In the case of the 14 mm scaffold, the scaffold swelling was about 500% of initial scaffold weight (~70-90% of maximum swelling) within one hour (Fig. 4 A). In the case of the 6 mm scaffold, the scaffold swelling, at all core contents tested, reached about 400% of initial scaffold weight (~90% of maximum swelling) already within one hour (Fig. 4 B). In all scaffolds tested, swelling in free environment reached more than 90% of maximum capacity within 8 hours.

1.3. Cytocompatibility of PU scaffold component material

Viable cell number after culture in the conditioned medium from both core and envelope material was >85% of control culture medium after up to 72 hours of culture for NPCs and MSCs (Fig. 5 A and B). Conditioned medium from core material supported MSC proliferation (viable cell number was above 160-180% of positive control after 72 hours culture), but did not affect NPC proliferation (viable cell number was 85-90% of positive control after 72 hours culture).

DNA content of cell-envelope constructs after 1 day of culture showed that 88% of the seeded cells were attached to the envelope 24 hours after seeding, suggesting high cell attachment ratio. Compared with day 1, the DNA content of samples increased 4-fold after 7 days of culture, indicating active NPC proliferation on the envelope (data not shown). Representative SEM images also showed that cells

seeded on the top side of the envelope had proliferated and produced extracellular matrix after 7 days of culture (Fig. 5 C).

2. IVD organ culture - mechanical effect of PU scaffold in nucleotomized IVD after 1 day of dynamic load

The implanted PU scaffold was able to entrap water and swell *in situ* (Fig. 6 A), as indicated by weight increase of $301\pm33\%$ and thickness increase of $103\pm15\%$ already after 24 h culture in the IVD.

After nucleotomy, the dynamic compressive stiffness modulus dropped to 30% compared with intact IVDs. After refilling the NP cavity with PU scaffold and free swelling culture overnight, the disc stiffness modulus was restored to $73\pm21\%$ ($p=0.073$ vs. empty control). After dynamic load and free swelling recovery the stiffness modulus of PU scaffold refilled IVDs further increased to $82\pm14\%$ ($p<0.05$ vs. empty control) (Fig. 6 B). Representative stress/strain curves of the empty control and PU scaffold refilled IVDs are shown in Figure 6 D and E respectively.

Nucleotomy caused 3% decrease in disc height compared to intact IVDs. After dynamic load, IVDs implanted with PU scaffold maintained their disc height, while the disc height of empty controls further dropped by 7% ($p<0.001$ vs. implant group). After free swelling recovery overnight, the disc height of the implant group was restored to the level of the intact IVDs ($p<0.001$ vs. empty control) (Fig. 6 C).

3. IVD organ culture – mechanical and biological effect of PU scaffold in nucleotomized IVD after 14 days of dynamic load

3.1. Disc height change

After the 1st cycle of dynamic load, a disc height loss of -9.8 ± 2.3 % was noticed in partially nucleotomized IVDs compared with initial dimension of respective intact IVDs after dissection (Fig. 7 A; Empty Day 1). Implantation of PU scaffold restored disc height to -2.1 ± 0.5 % (Fig. 7 A; Scaffold Day 1; $p < 0.05$ vs. Empty). After free swelling recovery, all the IVDs swelled and recovered to the height before load. The differences between partially nucleotomized IVDs and PU scaffold implanted IVDs were maintained. This diurnal disc height change pattern was observed during the entire period of 14 days repetitive dynamic load (Fig. 7 A).

3.2. Gene expression

After 14 days of culture with dynamic load, gene expression levels of NP and AF tissues were compared to the expression levels of disc tissues from respective bovine tails before starting organ culture on day 0 (Fig. 7 B and C). Compared with day 0, gene expression of IVD extracellular matrix components ACAN, COL2A1, COL1A2, BGN and Versican in partially nucleotomized IVDs (Empty) did not change significantly. Implantation of PU scaffold into the partially nucleotomized IVDs (Scaffold) also did not affect the expression level of these genes. Compared with healthy tissue of intact IVDs on day 0, gene expression of MMP13 in NP and AF tissues of partially nucleotomized IVDs increased 24-fold and 134-fold respectively after 14 days of culture with dynamic load. Implantation of PU scaffold into partially nucleotomized IVDs down-regulated the MMP13 gene expression in NP and AF by 8-fold and 7-fold, respectively compared with Empty group.

3.3. Biochemical analysis of disc tissue

GAG content, collagen content and proteoglycan synthesis rate per cell of native NP and AF tissues after 14 days of culture are shown in Table 4. In the remaining NP tissue after partial nucleotomy, GAG, collagen content and proteoglycan synthesis rate were not affected by implantation of the PU scaffold. In the AF tissue, neither GAG content nor collagen content per cell was affected by PU scaffold implantation.

3.4. Histological analysis of whole IVDs

Images of Safranin O/Fast Green stained sections of IVDs cultured for 14 days are shown in Fig. 8. The overview images (Fig. 8 A, C) clearly show that a partial nucleotomy was performed in the organ culture model. The swollen PU scaffold completely filled the nucleotomized region (Fig. 8 C). The envelope of the PU scaffold was observed as a ring in direct contact with the remaining disc NP tissue (Fig. 8 D). The remaining native disc NP tissue is still intensely stained with Safranin O after 14 days of dynamic load.

3.5. FTIR imaging analysis of discs tissue

An example of an image reflecting the tissue distribution (sagittal direction) of a partially nucleotomized IVD cultured for 14 days under dynamic load without PU scaffold implantation is shown in Fig. 9 A. Tissue distribution maps of ROI of partially nucleotomized IVDs without (top) and with (bottom) PU scaffold implantation cultured for 14 days under dynamic load are shown in Fig. 9 B. The ROI tissue image of the empty IVD shows fissures caused by the nucleotomy and native tissue across the whole width of the IVD. The ROI tissue image of the PU implanted IVD shows a cavity in the center of the IVD where the implant was situated, surrounded by native disc tissue. Estimated component / tissue distribution line profiles of proteoglycan,

collagen type II and collagen type I across the IVD sections show distinctive trends, with proteoglycan and collagen type II profiles showing an overall increase and collagen type I profiles showing a decrease towards the NP region (Fig. 9 C). A comparison of the line profiles between the empty and PU scaffold implanted IVD shows very similar overall trends for proteoglycan, collagen type II and collagen type I. However, both proteoglycan and collagen type II show localized higher component to tissue ratios (sharp positive features) at around 25 %, 30 % and 67 % IVD width in the PU implanted IVDs. Collagen type I line profiles show localized lower component to tissue ratios (sharp negative features) at around the same areas (25 %, 30 % and 67 % IVD width) in the PU implanted IVDs.

Discussion

The aim of this study was to develop a nucleus pulposus replacement material, which is feasible for non-invasive delivery and custom-made design, restores the mechanical property of nucleotomized IVDs and sustains cytocompatibility at the same time. The bi-phasic PU scaffold developed in this work has a flat discoid shape after manufacturing (Fig. 1 A front) and will swell after insertion into the IVD. Swelling rate is important for scaffold development and implementation, and enables the selection of the optimal core content. The PU scaffolds showed favorable *in vitro* swelling capability (Fig. 3 and Table 2) with a fast swelling rate (Fig. 4) post-hydration. Based on these results the extent of swelling could be tailored to the desired external scaffold dimensions. Hence a custom-made design is feasible depending on the individual geometry of NP material to be replaced. Implantation of the PU scaffolds into nucleotomized IVDs further confirmed the swelling capability of the PU scaffolds *in situ*. The implanted PU scaffolds expanded anisotropically to fill the nucleotomy

defect (Fig. 6 A and Fig. 8 C). In addition, stress relaxation tests revealed higher toe and linear modulus for these PU scaffolds than for human NP and no significant difference in percentage relaxation between the PU scaffold and human NP, further indicating the suitability of the material for NP replacement (unpublished results from consortium partner).

The cytocompatibility of the PU scaffold was assessed with NP cells and bone marrow derived MSCs. Viable cell numbers after culturing in the conditioned medium from the core or the envelope material were higher than 85% of cell numbers after culture in control medium (Fig. 5 A and B). In addition, NP cells were seeded on top of the outer envelope material, and presented effective adhesion after 1 day and active cell proliferation and extracellular matrix synthesis after 7 days (Fig. 5 C). These results indicate that the cytocompatibility of the PU scaffolds is advantageous with respect to both NP cells and MSCs. Another interesting finding is that the conditioned medium of the core material stimulated MSC growth compared to the control medium. The underlying reason of this observation should be further examined in future studies.

The main challenge in developing an NP replacement material is to immediately restore the mechanical property in a nucleotomized IVD. Emerging numbers of NP replacement devices/biomaterials have been tested for their mechanical restoration effect in nucleotomized IVDs [9, 34-37]. However, all the materials were tested in *ex vivo* or *in vivo* nucleotomy models with an incision through the AF. Reitmaier *et al.* compared two annulus closure methods after NP replacement with the native NP tissue removed during nucleotomy. They found that the disc height loss and disc stiffness differ between the two conditions. This demonstrates that the preservation of the disc's mechanical function following NP replacement is partially dependent on the

quality of the closure of the annulus defect [38]. This may also explain some failures of NP replacement materials in the case of dislocation or protrusion through the AF incision. To assess the mechanical repair effect of the NP replacement material solely, an alternative nucleotomy approach in organ culture was used in this study, whereby an incision was made through the endplate while preserving an intact annulus (Fig. 6 A right) [22]. This model is highly useful for evaluation and screening NP replacement materials in whole organ culture under load before pre-clinical *in vivo* testing.

In the current study, partial nucleotomy through the endplate in the organ cultured IVD substantially altered the mechanical property of the IVD, as indicated by a 70% reduction in the axial stiffness (Fig. 6 B). Implantation of the PU scaffold significantly restored the axial stiffness and disc height of the nucleotomized IVD after cyclic dynamic load and recovery culture (Fig. 6 B and C). The restoration in axial stiffness and disc height occurred relatively fast, already after the first cycle of 3 hours load, which indicates an immediate repair effect. Furthermore, the disc height restoration was maintained through 14 days of repetitive dynamic load and recovery culture (Fig. 7 A), which indicates that the PU scaffolds implanted *in situ* are able to restore the mechanical property of a nucleotomized IVD in organ culture. In our previous study [22], a fibrin-hyaluronan hydrogel was delivered into nucleotomized IVD and the mechanical repair function was assessed with the same method. It was found that the fibrin-hyaluronan hydrogel restored the disc height after dynamic loading, but not the dynamic compressive stiffness of the nucleotomized IVD. These results demonstrate that the PU scaffolds developed in this study are superiorly able to restore the mechanical function of the nucleotomized IVD compared to a biomimetic hydrogel. In the current study, the mechanical characterization was focused on the compressive modulus and the disc height change. The assessment of the

viscoelastic parameters and the neutral zone of the IVD before and after scaffold implantation will also be of interest for us in future studies to explore the effects of the scaffolds in more detail.

Another advantage of our organ culture model is that the IVDs can be maintained viable under dynamic load in a bioreactor for several weeks [25], after which the biological property of the nucleotomized IVDs with/without NP replacement can be assessed. In this study, after 14 days culture with dynamic load, we investigated the phenotype of the disc cells, the extracellular matrix components, and the structure of the disc tissue in nucleotomized IVDs with/without implanted PU scaffold. In nucleotomized IVDs without NP replacement, the MMP13 gene expression level of the cells in the AF tissue and remaining NP tissue increased dramatically after 14 days of culture (Fig. 7 B and C), which demonstrates an increase in catabolic signals in the disc tissue. MMP13 is known to be overexpressed in cartilage from patients with osteoarthritis compared with healthy cartilage [39]. The expression and activity of MMP13 are also increased during disc degeneration [40]. This indicates that a IVD after partial nucleotomy is prone to a degenerative pathology in the remaining native disc tissue. Implantation of the PU scaffold into the nucleotomized IVD markedly down-regulated the MMP13 expression in the NP and AF tissues (Fig. 7 B and C). This may slow down further degeneration of the native disc tissue compared with the unrepaired IVD.

The content and distribution of proteoglycan and collagen in the disc tissue were analyzed by biochemical measurement, Safranin O/Fast Green staining, and FTIR on disc sections. The disc matrix composition was not changed significantly in the NP and AF regions of the IVDs in the presence of the PU scaffold. However, in the native NP tissue surrounding the implanted PU scaffold, proteoglycan and type II collagen

showed localized higher expression, while type I collagen showed localized lower expression compared with the nucleotomized IVD without repair (Fig. 9 C). This indicates that the implanted PU scaffold is beneficial in maintaining the NP cell phenotype in the surrounded disc tissue.

The underlying reason for the above mentioned biological changes is likely to result from the restoration in the geometry and load pressure on the remaining native disc tissue. In the nucleotomized IVD without repair, the remaining disc tissue swells into the nucleotomized region. Therefore, the tissue is less compact and the pressure on the tissue is disturbed. The implantation of the PU scaffold decreased the native tissue volume in the disc space by occupying the NP cavity, which is likely to lead to a higher local intensity of proteoglycan and type II collagen. Furthermore, the implanted PU scaffold restored the pressure in the nucleotomized region and the stiffness of the IVD, therefore the remaining disc tissue experienced higher load pressure compared with the tissue in the non-repaired IVD. Our previous study has shown that dynamic load down-regulated the MMP13 gene expression level in AF tissue and COL1 gene expression level in NP tissue from organ cultured IVD compared with free swelling condition [27]. Other *ex vivo* studies also revealed that dynamic load preserves disc cell phenotype compared to unloaded or static load condition [41, 42]. Taken together, these data corroborate that mechanical pressure is essential to maintain the function and homeostasis of the disc tissue. The PU scaffold developed in this study, as an NP replacement material, can rebalance the pressure in the nucleotomized IVD and has the potential to prevent further degeneration of the remaining disc tissue.

The dry PU scaffolds can be rolled into a tube and delivered through a needle with insertion guide (Fig. 1 C). Such injectable design allows less invasive delivery

649 compared to the mechanical NP replacement devices, including NUBAC™ [43],
650 REGAIN™ [34], and BUCK™ [9]. Furthermore, a transpedicular approach has
651 recently been developed to deliver therapeutic factors to the IVD without further
652 damage to the AF [44, 45]. With this approach, our PU scaffolds could be delivered
653 through the pedicle and the endplate to the NP while preserving the mechanical
654 function of AF in cases of early disc degeneration with an intact annulus. In case of
655 patients with AF defects, proper AF closure approach is needed to prevent herniation
656 of the implanted NP replacement material. Suture [46] and glue [47, 48] may be
657 sufficient to close small annular defects. For large annular failure, tissue engineered
658 material mimicking native AF tissue may be needed to fully restore the mechanical
659 property of the AF [27]. Regardless of mechanical properties, the nucleotomy
660 approach through the endplate might also induce a biological degenerative cascade
661 according to literature data. Damage of the EP by drilling has been shown to
662 decrease the water content in the outer AF and proteoglycan content in the NP [49]
663 and may trigger Schmorl's nodes [45]. Further investigation to optimize the
664 transpedicular approach is essential to fully reach the requirements of a safe, non-
665 invasive, and functional NP replacement therapy.

666 Limitations of the current study remain in the following aspects: 1) the PU scaffolds
667 were assessed in nucleotomized IVD under healthy conditions; hence exposure to
668 the pathological environment occurring in a degenerative IVD is lacking; 2) the *ex*
669 *vivo* organ culture model differs from *in vivo* conditions where additional systemic
670 responses may arise. More research work will therefore be necessary to assess the
671 effects of the material before clinical translation can be considered. Whole organ
672 culture models mimicking IVD degeneration through enzymatic treatment of the NP
673 [50, 51], high frequency mechanical loading [52], or addition of pro-inflammatory
674 cytokines [53] may be used to evaluate the material under pathological conditions.

Ultimately, *in vivo* large animal models would provide further insight into the delivery, stability and effect of the PU scaffolds for NP replacement at longer term after implantation.

Conclusions

In this study, an injectable and cytocompatible bi-phasic PU scaffold was developed for NP replacement. The implant was assessed in whole organ culture under dynamic load for its mechanical and biological repair effect in nucleotomized IVD. The nucleotomy model through the endplate enabled pure assessment of the PU scaffold, independent of the closure method for an annulus incision. The designed PU scaffold with swelling capacity *in situ* is able to restore the mechanical property of nucleotomized IVDs, and shows potential to retard further degeneration of native disc tissue. This work provides a new approach to facilitate future progress in the development of an NP replacement material, and the screening of materials using whole organ culture. The bi-phasic PU scaffold developed in the current study warrants further pre-clinical investigation to evaluate its potential for functional, non-invasive and custom designed NP replacement.

Acknowledgement

This study was funded by the European Commission under the FP7-NMP project Npmimetic (246351). We thank Peter Kinast (Melab Medizintechnik und Labor GmbH, Germany) for providing the needle delivery system.

References

1. Pattappa G, Li Z, Peroglio M, Wismer N, Alini M, Grad S. Diversity of intervertebral disc cells: phenotype and function. *J Anat* 2012;221:480-496.
2. Adams MA, Roughley PJ. What is intervertebral disc degeneration, and what causes it? *Spine (Phila Pa 1976)* 2006;31:2151-2161.
3. Mok FP, Samartzis D, Karppinen J, Fong DY, Luk KD, Cheung KM. Modic changes of the lumbar spine: prevalence, risk factors, and association with disc degeneration and low back pain in a large-scale population-based cohort. *Spine J* 2016;16:32-41.
4. Spoor AB, Oner FC. Minimally invasive spine surgery in chronic low back pain patients. *J Neurosurg Sci* 2013;57:203-218.
5. Park P, Garton HJ, Gala VC, Hoff JT, McGillicuddy JE. Adjacent segment disease after lumbar or lumbosacral fusion: review of the literature. *Spine (Phila Pa 1976)* 2004;29:1938-1944.
6. Jacobs WC, van der Gaag NA, Kruijt MC, Tuschel A, de Kleuver M, Peul WC, et al. Total disc replacement for chronic discogenic low back pain: a Cochrane review. *Spine (Phila Pa 1976)* 2013;38:24-36.
7. Roberts S, Evans H, Trivedi J, Menage J. Histology and pathology of the human intervertebral disc. *J Bone Joint Surg Am* 2006;88 Suppl 2:10-14.
8. Roughley PJ. Biology of intervertebral disc aging and degeneration: involvement of the extracellular matrix. *Spine (Phila Pa 1976)* 2004;29:2691-2699.
9. Lewis G. Nucleus pulposus replacement and regeneration/repair technologies: present status and future prospects. *J Biomed Mater Res B Appl Biomater* 2012;100:1702-1720.

10. Balkovec C, Vernengo J, McGill SM. The use of a novel injectable hydrogel nucleus pulposus replacement in restoring the mechanical properties of cyclically fatigued porcine intervertebral discs. *J Biomech Eng* 2013;135:61004-61005.
11. Borges AC, Eyholzer C, Duc F, Bourban PE, Tingaut P, Zimmermann T, et al. Nanofibrillated cellulose composite hydrogel for the replacement of the nucleus pulposus. *Acta Biomater* 2011;7:3412-3421.
12. Cannella M, Isaacs JL, Allen S, Orana A, Vresilovic E, Marcolongo M. Nucleus implantation: the biomechanics of augmentation versus replacement with varying degrees of nucleotomy. *J Biomech Eng* 2014;136:051001.
13. Showalter BL, Elliott DM, Chen W, Malhotra NR. Evaluation of an In Situ Gelable and Injectable Hydrogel Treatment to Preserve Human Disc Mechanical Function Undergoing Physiologic Cyclic Loading Followed by Hydrated Recovery. *J Biomech Eng* 2015;137:081008.
14. Allen MJ, Schoonmaker JE, Bauer TW, Williams PF, Higham PA, Yuan HA. Preclinical evaluation of a poly (vinyl alcohol) hydrogel implant as a replacement for the nucleus pulposus. *Spine (Phila Pa 1976)* 2004;29:515-523.
15. Smolders LA, Bergknut N, Kingma I, van der Veen AJ, Smit TH, Koole LH, et al. Biomechanical evaluation of a novel nucleus pulposus prosthesis in canine cadaveric spines. *Vet J* 2012;192:199-205.
16. Zhang ZM, Zhao L, Qu DB, Jin DD. Artificial nucleus replacement: surgical and clinical experience. *Orthop Surg* 2009;1:52-57.
17. Lamba NMK, Woodhouse KA, Cooper SL. Polyurethanes in biomedical applications: CRC Press; 1998, pp. 205-255.
18. Skorkowska-Telichowska K, Czemplik M, Kulma A, Szopa J. The local treatment and available dressings designed for chronic wounds. *J Am Acad Dermatol* 2013;68:e117-126.

19. Chandy T, Van Hee J, Nettekoven W, Johnson J. Long-term in vitro stability assessment of polycarbonate urethane micro catheters: resistance to oxidation and stress cracking. *J Biomed Mater Res B Appl Biomater* 2009;89:314-324.
20. Yang M, Zhang Z, Hahn C, Laroche G, King MW, Guidoin R. Totally implantable artificial hearts and left ventricular assist devices: selecting impermeable polycarbonate urethane to manufacture ventricles. *J Biomed Mater Res* 1999;48:13-23.
21. St John KR. The use of polyurethane materials in the surgery of the spine: a review. *Spine J* 2014;14:3038-3047.
22. Li Z, Kaplan KM, Wertz A, Peroglio M, Amit B, Alini M, et al. Biomimetic fibrin-hyaluronan hydrogels for nucleus pulposus regeneration. *Regen Med* 2014;9:309-326.
23. Li Z, Kupcsik L, Yao SJ, Alini M, Stoddart MJ. Chondrogenesis of human bone marrow mesenchymal stem cells in fibrin-polyurethane composites. *Tissue Eng Part A* 2009;15:1729-1737.
24. Peroglio M, Grad S, Mortisen D, Sprecher CM, Illien-Junger S, Alini M, et al. Injectable thermoreversible hyaluronan-based hydrogels for nucleus pulposus cell encapsulation. *Eur Spine J* 2012;21 Suppl 6:S839-849.
25. Juenger S, Gantenbein-Ritter B, Lezuo P, Ferguson S, Alini M, Ito K. Effect of limited nutrition on in situ intervertebral disc cells under simulated-physiological loading. *Spine* 2009;34:1264-1271.
26. Botsford DJ, Esses SI, Ogilvie-Harris DJ. In vivo diurnal variation in intervertebral disc volume and morphology. *Spine (Phila Pa 1976)* 1994;19:935-940.
27. Pirvu T, Blanquer SB, Benneker LM, Grijpma DW, Richards RG, Alini M, et al. A combined biomaterial and cellular approach for annulus fibrosus rupture repair. *Biomaterials* 2015;42:11-19.

28. Farndale RW, Buttle DJ, Barrett AJ. Improved quantitation and discrimination of sulphated glycosaminoglycans by use of dimethylmethylene blue. *Biochim Biophys Acta* 1986;883:173-177.
29. Wismer N, Grad S, Fortunato G, Ferguson SJ, Alini M, Eglin D. Biodegradable electrospun scaffolds for annulus fibrosus tissue engineering: effect of scaffold structure and composition on annulus fibrosus cells in vitro. *Tissue Eng Part A* 2014;20:672-682.
30. Rieppo L, Saarakkala S, Narhi T, Helminen HJ, Jurvelin JS, Rieppo J. Application of second derivative spectroscopy for increasing molecular specificity of Fourier transform infrared spectroscopic imaging of articular cartilage. *Osteoarthritis Cartilage* 2012;20:451-459.
31. Andrew JJ, Hancewicz TM. Rapid analysis of raman image data using two-way-multivariate curve resolution. *Applied Spectroscopy* 1998;52:797-807.
32. Wang JH, Hopke PK, Hancewicz TM, Zhang SL. Application of modified alternating least squares regression to spectroscopic image analysis. *Anal Chim Acta* 2003;476:93-109.
33. Mader KT, Le Maitre CL, Sammom C. Characterisation of intervertebral discs using MID-IR spectroscopic imaging. *Global Spine J* 2014;04:58.
34. Coric D, Mummaneni PV. Nucleus replacement technologies. *J Neurosurg Spine* 2008;8:115-120.
35. Buser Z, Kuelling F, Liu J, Liebenberg E, Thorne KJ, Coughlin D, et al. Biological and biomechanical effects of fibrin injection into porcine intervertebral discs. *Spine (Phila Pa 1976)* 2011;36:E1201-1209.
36. Hegewald AA, Knecht S, Baumgartner D, Gerber H, Endres M, Kaps C, et al. Biomechanical testing of a polymer-based biomaterial for the restoration of spinal stability after nucleotomy. *J Orthop Surg Res* 2009;4:25.

37. Huang B, Zhuang Y, Li CQ, Liu LT, Zhou Y. Regeneration of the intervertebral disc with nucleus pulposus cell-seeded collagen II/hyaluronan/chondroitin-6-sulfate tri-copolymer constructs in a rabbit disc degeneration model. *Spine (Phila Pa 1976)* 2011;36:2252-2259.
38. Reitmaier S, Shirazi-Adl A, Bashkuev M, Wilke HJ, Gloria A, Schmidt H. In vitro and in silico investigations of disc nucleus replacement. *J R Soc Interface* 2012;9:1869-1879.
39. Aref-Eshghi E, Liu M, Harper PE, Dore J, Martin G, Furey A, et al. Overexpression of MMP13 in human osteoarthritic cartilage is associated with the SMAD-independent TGF-beta signalling pathway. *Arthritis Res Ther* 2015;17:264.
40. Le Maitre CL, Freemont AJ, Hoyland JA. Localization of degradative enzymes and their inhibitors in the degenerate human intervertebral disc. *J Pathol* 2004;204:47-54.
41. Paul CP, Zuiderbaan HA, Zandieh Doulabi B, van der Veen AJ, van de Ven PM, Smit TH, et al. Simulated-physiological loading conditions preserve biological and mechanical properties of caprine lumbar intervertebral discs in ex vivo culture. *PLoS One* 2012;7:e33147.
42. Wang DL, Jiang SD, Dai LY. Biologic response of the intervertebral disc to static and dynamic compression in vitro. *Spine (Phila Pa 1976)* 2007;32:2521-2528.
43. Balsano M, Zachos A, Ruggiu A, Barca F, Tranquilli-Leali P, Doria C. Nucleus disc arthroplasty with the NUBAC device: 2-year clinical experience. *Eur Spine J* 2011;20 Suppl 1:S36-40.
44. Vadala G, De Strobel F, Bernardini M, Denaro L, D'Avella D, Denaro V. The transpedicular approach for the study of intervertebral disc regeneration strategies: in vivo characterization. *Eur Spine J* 2013;22 Suppl 6:S972-978.

45. Vadala G, Russo F, Pattappa G, Schiuma D, Peroglio M, Benneker LM, et al. The transpedicular approach as an alternative route for intervertebral disc regeneration. Spine (Phila Pa 1976) 2013;38:E319-324.
46. Chiang CJ, Cheng CK, Sun JS, Liao CJ, Wang YH, Tsuang YH. The effect of a new anular repair after discectomy in intervertebral disc degeneration: an experimental study using a porcine spine model. Spine (Phila Pa 1976) 2011;36:761-769.
47. Grunert P, Borde BH, Hudson KD, Macielak MR, Bonassar LJ, Hartl R. Annular repair using high-density collagen gel: a rat-tail in vivo model. Spine (Phila Pa 1976) 2014;39:198-206.
48. Guterl CC, Torre OM, Purmessur D, Dave K, Likhitpanichkul M, Hecht AC, et al. Characterization of mechanics and cytocompatibility of fibrin-genipin annulus fibrosus sealant with the addition of cell adhesion molecules. Tissue Eng Part A 2014;20:2536-2545.
49. Holm S, Holm AK, Ekstrom L, Karladani A, Hansson T. Experimental disc degeneration due to endplate injury. J Spinal Disord Tech 2004;17:64-71.
50. Chan SC, Burki A, Bonel HM, Benneker LM, Gantenbein-Ritter B. Papain-induced in vitro disc degeneration model for the study of injectable nucleus pulposus therapy. Spine J 2013;13:273-283.
51. Jim B, Steffen T, Moir J, Roughley P, Haglund L. Development of an intact intervertebral disc organ culture system in which degeneration can be induced as a prelude to studying repair potential. Eur Spine J 2011;20:1244-1254.
52. Illien-Jünger S, Gantenbein-Ritter B, Grad S, Lezuo P, Ferguson SJ, Alini M, et al. The combined effects of limited nutrition and high frequency loading on intervertebral discs with endplates. Spine 2010;35:1744-1752.

850 53. Teixeira GQ, Boldt A, Nagl I, Pereira CL, Benz K, Wilke HJ, et al. A
851 Degenerative/Proinflammatory Intervertebral Disc Organ Culture: An Ex Vivo Model
852 for Anti-inflammatory Drug and Cell Therapy. Tissue Eng Part C Methods 2016;22:8-
853 19.

854

855

Table 1. The effect of Chronoflex™ (CF) : Hydromed™ (HM) w/w ratio on the function of the envelope material.

Experimental Group	CF:HM w/w ratio	Tensile Strength (N/mm ²)	Wetting time (minutes)
1	1:0	5.32	300
2	15:1	5.31	210
3	12:1	4.80	30
4	10:1	4.71	18
5	9:1	4.65	5
6	8:1	4.28	5
7	6:1	4.1	2
8	4:1	3.7	1

Table 2. Oligonucleotide primers and probes (bovine) used for real-time PCR.

Gene	Primer/probe type	Sequence
COL1A2	Primer fw (5'-3')	TGC AGT AAC TTC GTG CCT AGC A
	Primer rev (5'-3')	CGC GTG GTC CTC TAT CTC CA
	Probe (5'FAM/3'TAMRA)	CAT GCC AAT CCT TAC AAG AGG CAA CTG C
COL2A1	Primer fw (5'-3')	AAG AAA CAC ATC TGG TTT GGA GAA A
	Primer rev (5'-3')	TGG GAG CCA GGT TGT CAT C
	Probe (5'FAM/3'TAMRA)	CAA CGG TGG CTT CCA CTT CAG CTA TGG
ACAN	Primer fw (5'-3')	CCA ACG AAA CCT ATG ACG TGT ACT
	Primer rev (5'-3')	GCA CTC GTT GGC TGC CTC
	Probe (5'FAM/3'TAMRA)	ATG TTG CAT AGA AGA CCT CGC CCT CCA T
MMP13	Primer fw (5'-3')	CCA TCT ACA CCT ACA CTG GCA AAA
	Primer rev (5'-3')	GTC TGG CGT TTT GGG ATG TT
	Probe (5'FAM/3'TAMRA)	TCT CTC TAT GGT CCA GGA GAT GAA GAC CCC
ACAN: aggrecan; COL1A2: collagen type I; COL2A1: collagen type II; MMP13: matrix metalloproteinase 13; fw: Forward; rev: Reverse; FAM: Carboxyfluorescein; TAMRA: Tetramethylrhodamine		

Table 3. Swelling capacity (at saturation) of PU scaffolds with various sizes in aqueous media, Mean \pm SD.

Core content (mg)	Scaffold diameter (mm)	Increase in scaffold weight (% of initial)	Increase in core weight (% of initial)
3.4 (n=10)	6	409.96% \pm 21	825.68% \pm 34
4.5 (n=6)		444.49% \pm 25	769.40% \pm 17
12 (n=5)	8	563.07% \pm 26	783.01% \pm 40
12 (n=10)	9	559.22% \pm 18	847.85% \pm 20
40 (n=7)	14	635.40% \pm 13	846.20% \pm 25

Table 4. Biochemical analysis of native disc tissue in partially nucleotomized IVDs without/with PU scaffold implantation after 14 days of dynamic load. Total glycosaminoglycan (GAG) content, total collagen content and proteoglycan (PG) synthesis rate were measured and normalized to the DNA content of the respective samples. Empty – partially nucleotomized IVD, Scaffold – partially nucleotomized IVD implanted with PU scaffold. GAG/DNA ratio in $\mu\text{g} / \mu\text{g}$; Collagen/DNA ratio in $\mu\text{g} / \mu\text{g}$, PG/DNA in counts per minute (CPM) / μg ; PG/DNA was performed for NP tissue only. Mean \pm SD, n=6.

Biochemical analysis of disc tissue		
NP tissue		
Group	Empty	Scaffold
GAG / DNA	1151.6 \pm 224.7	1166.8 \pm 369.1
Collagen / DNA	639.9 \pm 474.3	1017.2 \pm 944.5
PG / DNA	98.4 \pm 45.1	79.1 \pm 50.2
AF tissue		
Group	Empty	Scaffold
GAG / DNA	628.9 \pm 348.1	502.8 \pm 281.2
Collagen / DNA	1070.4 \pm 653.9	1276.8 \pm 640.6

Figure1

[Click here to download high resolution image](#)

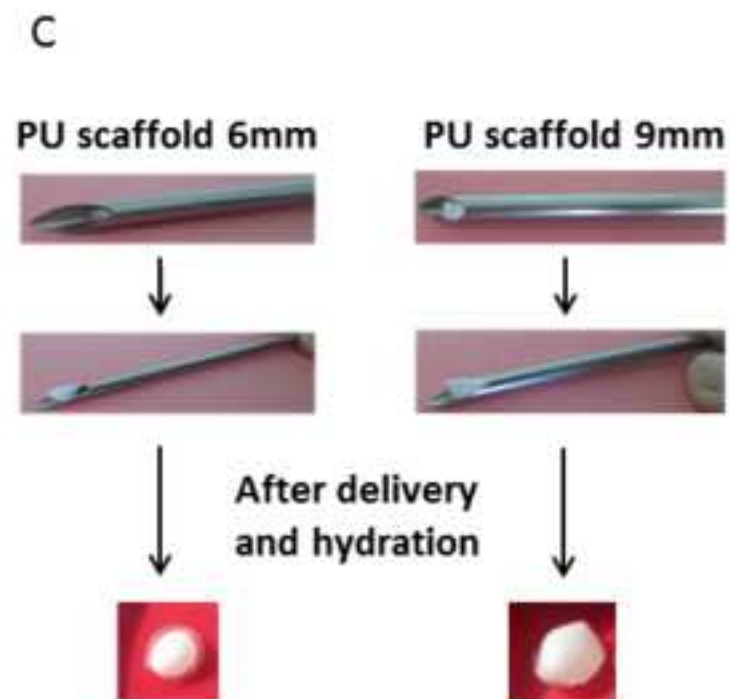
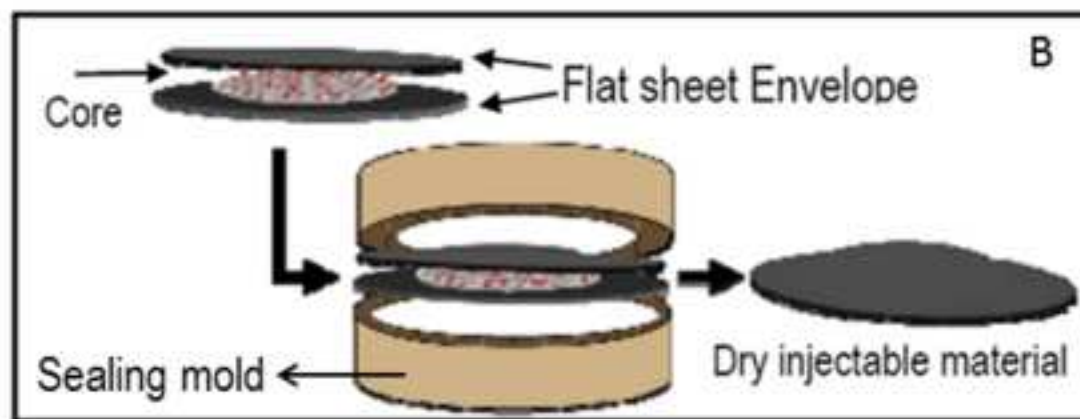
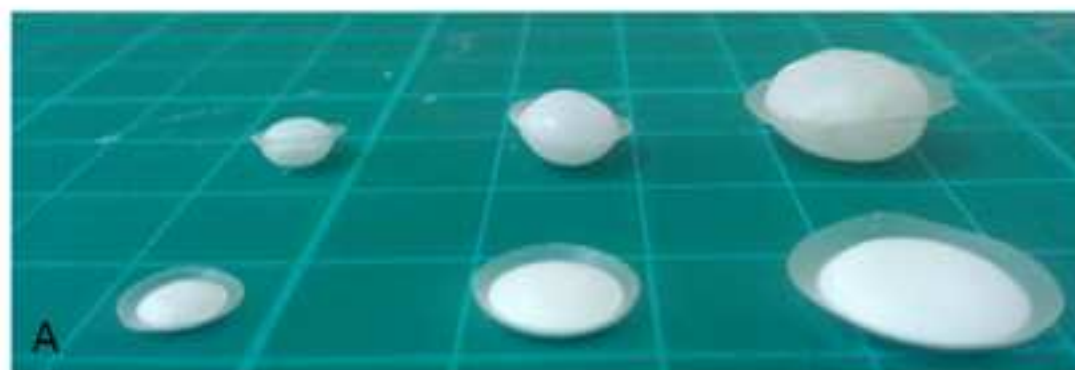


Figure 2
[Click here to download high resolution image](#)

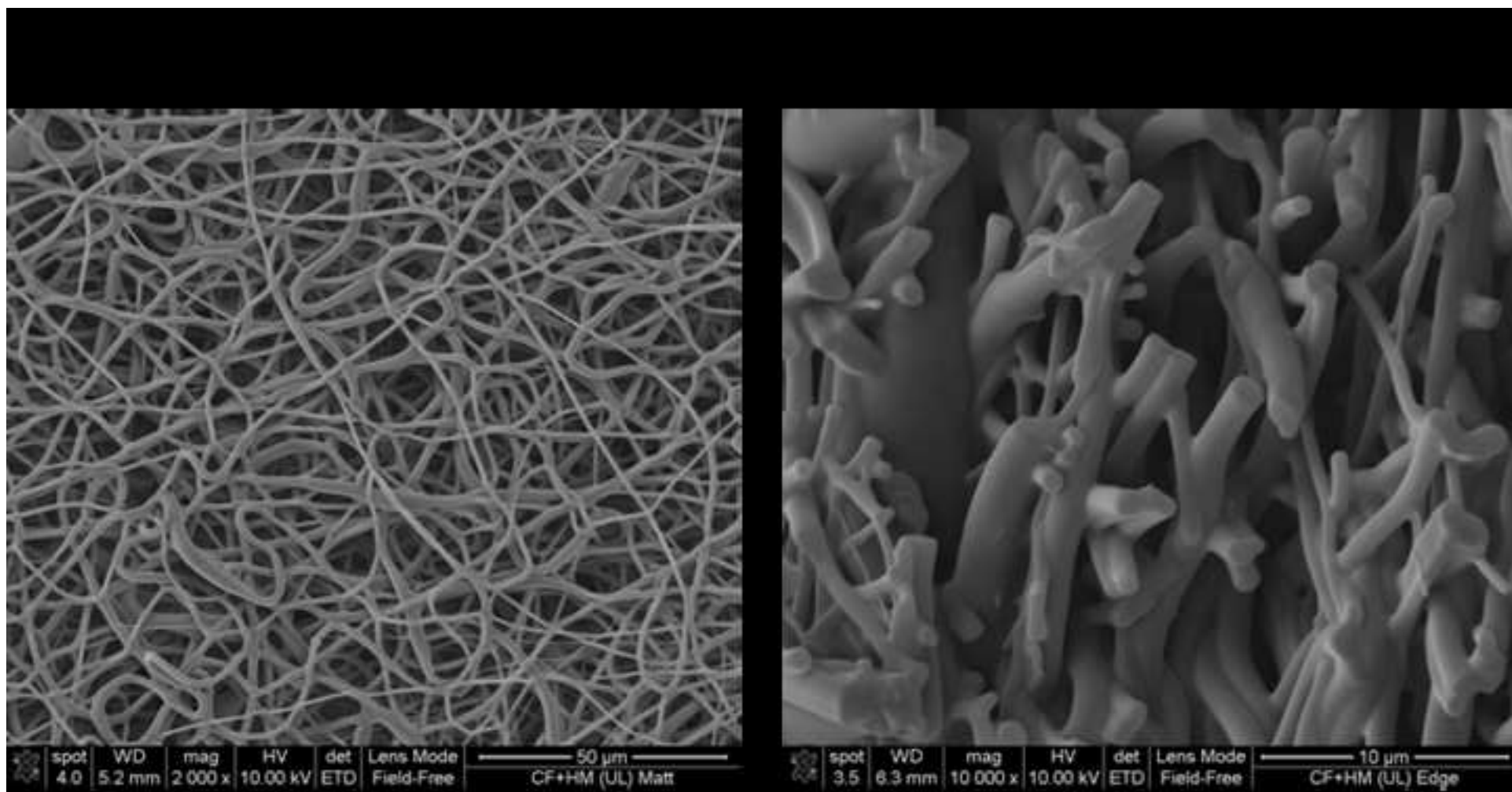


Figure 3
[Click here to download high resolution image](#)

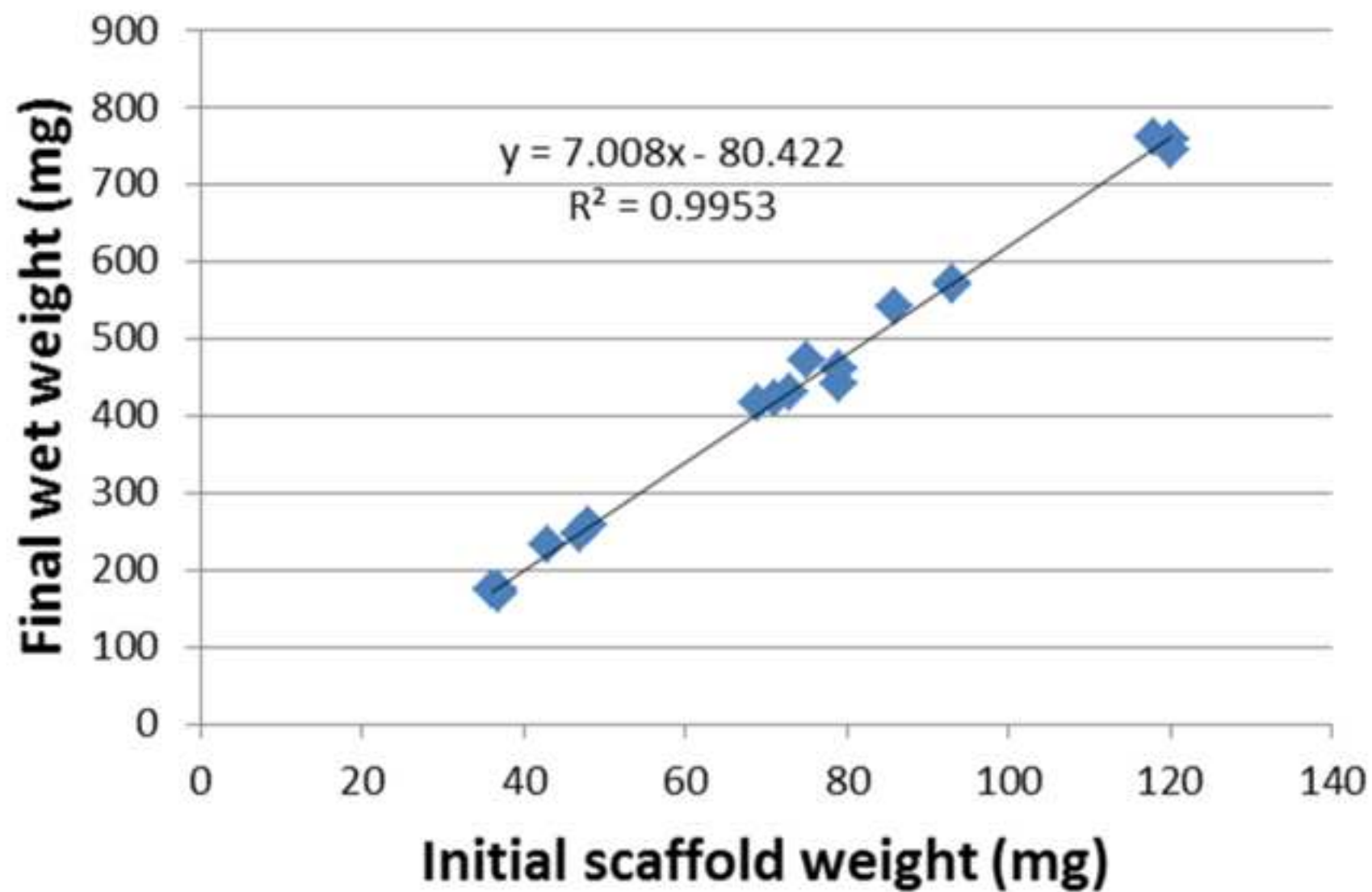


Figure 4
[Click here to download high resolution image](#)

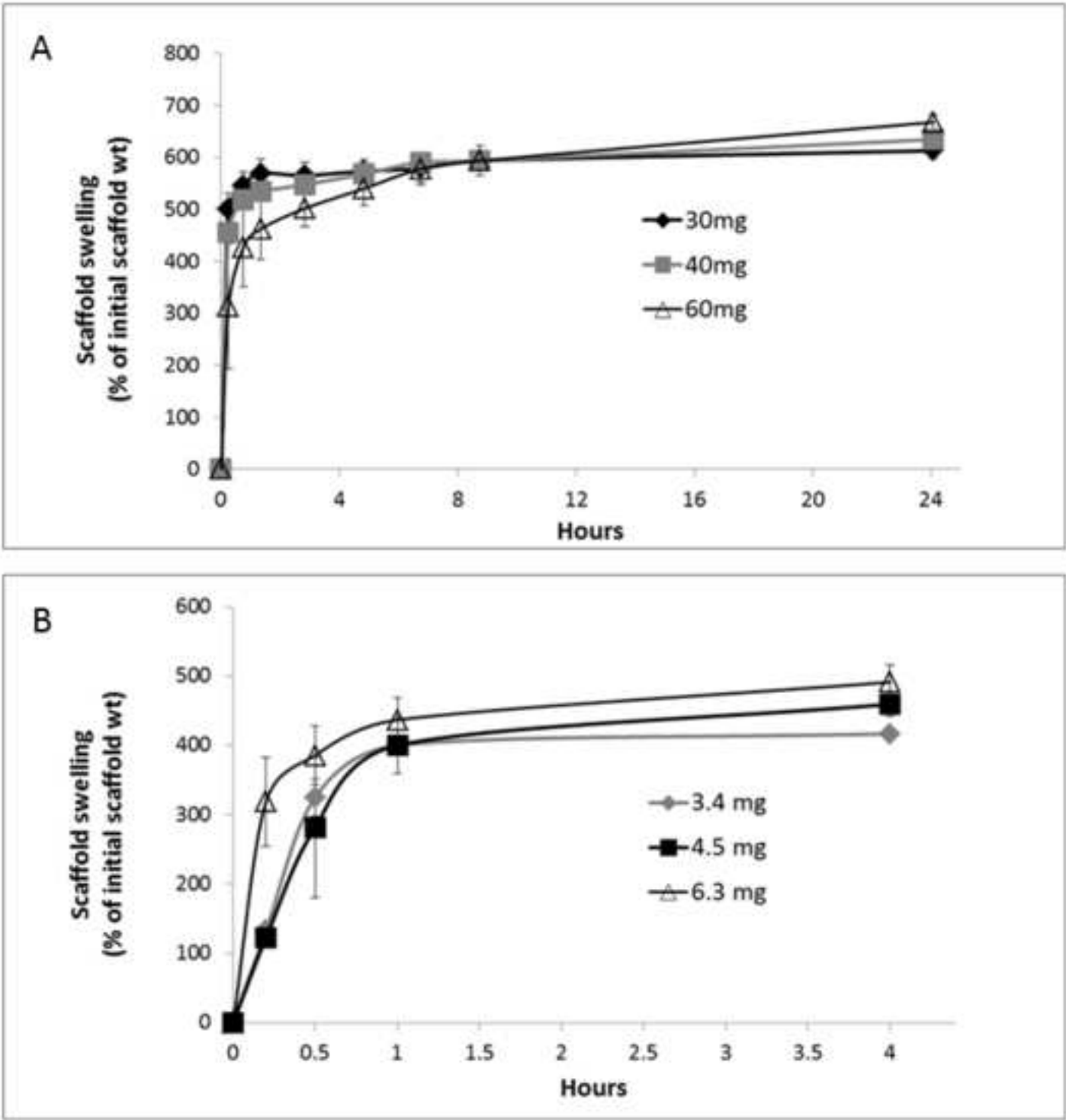


Figure 5
[Click here to download high resolution image](#)

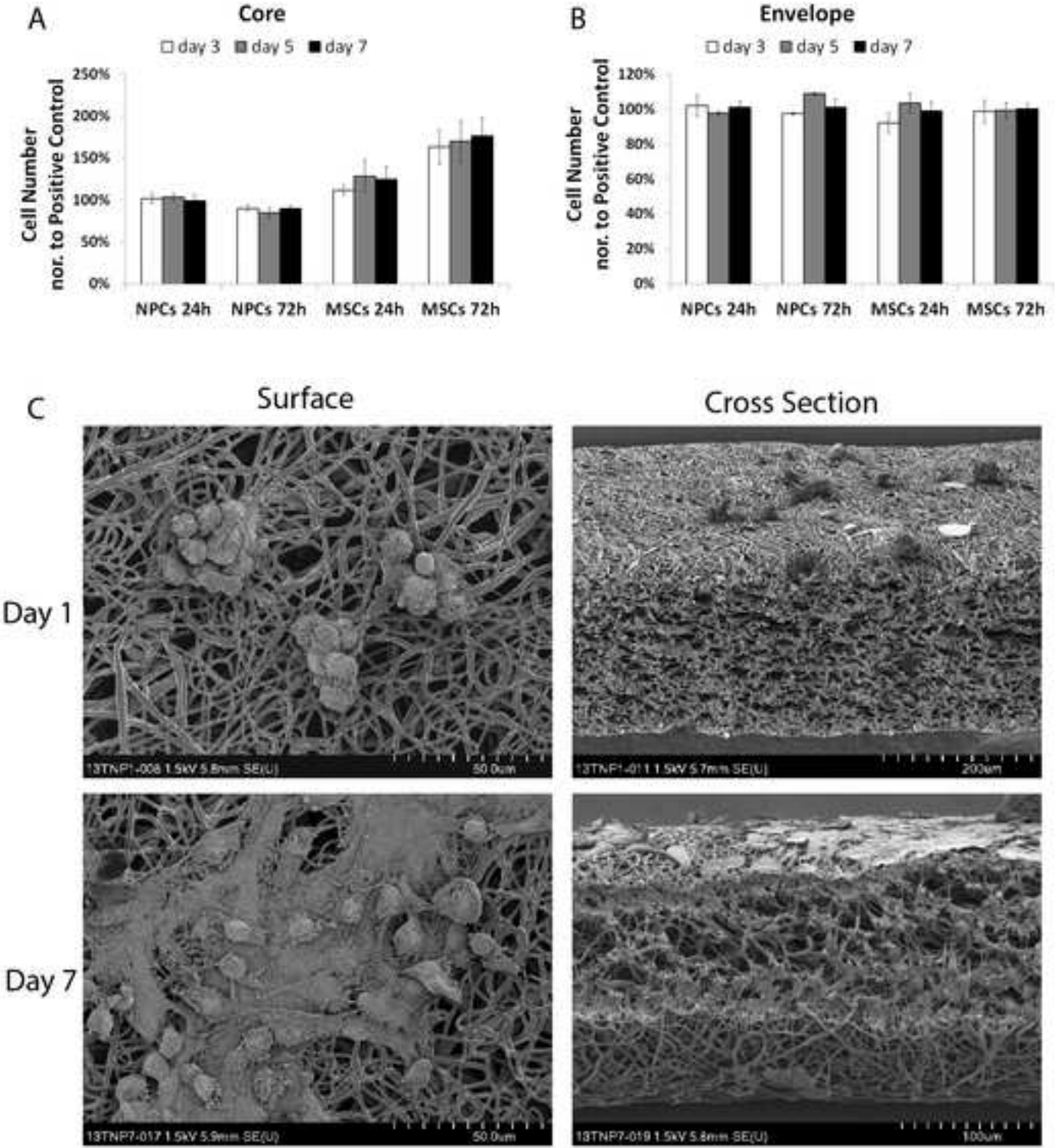


Figure6

[Click here to download high resolution image](#)

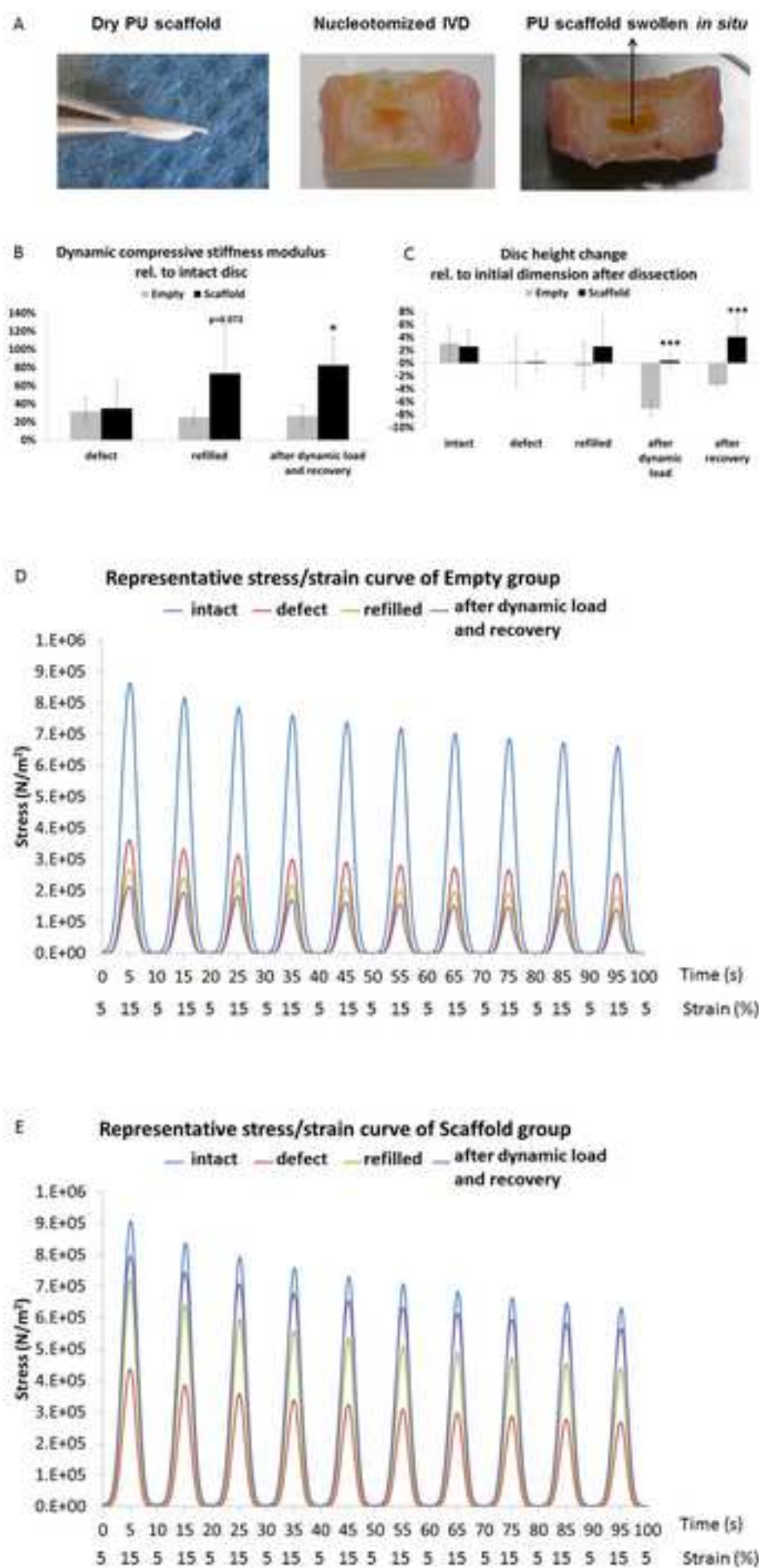


Figure7
[Click here to download high resolution image](#)

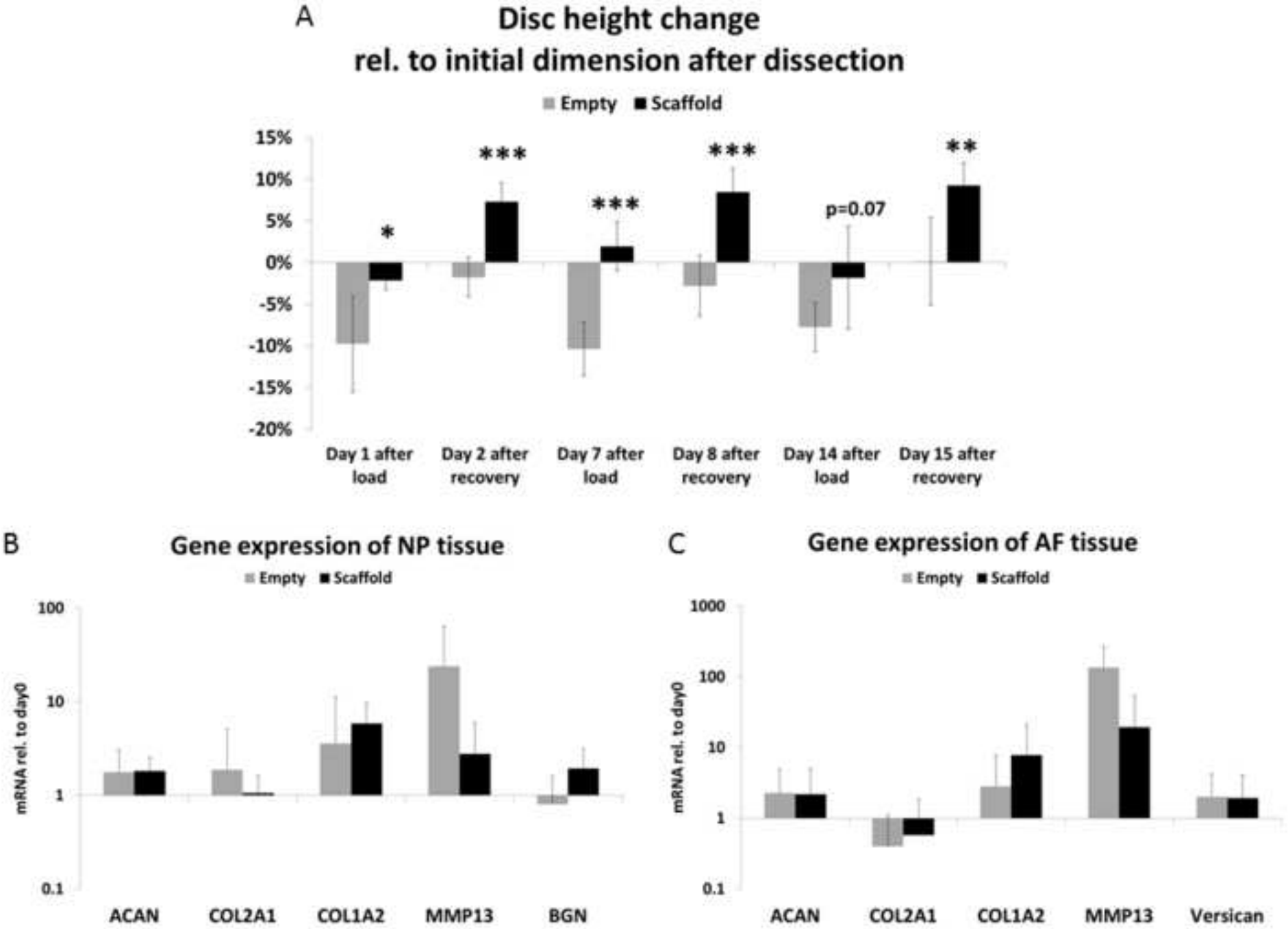


Figure 8
[Click here to download high resolution image](#)

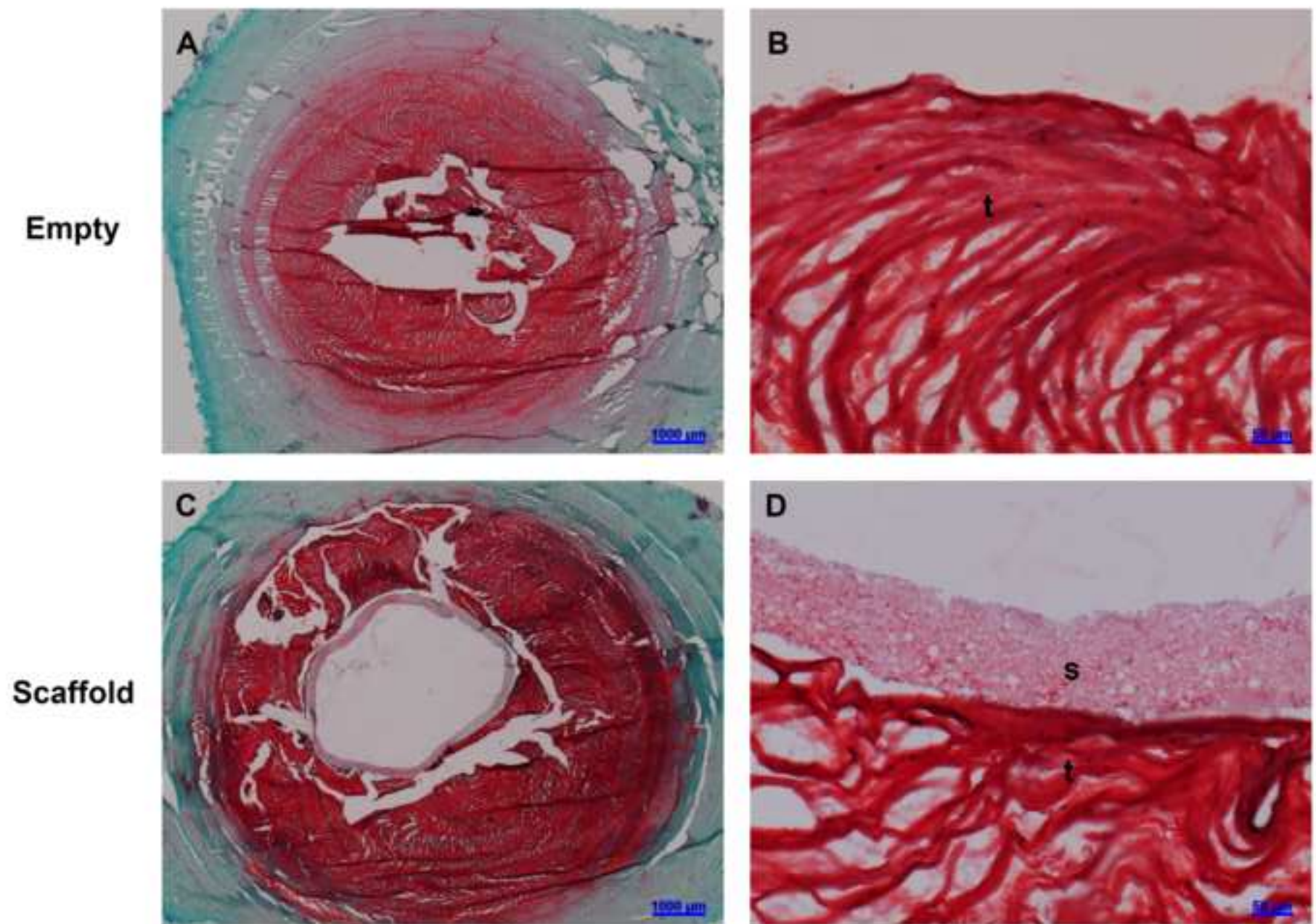


Figure 9
[Click here to download high resolution image](#)

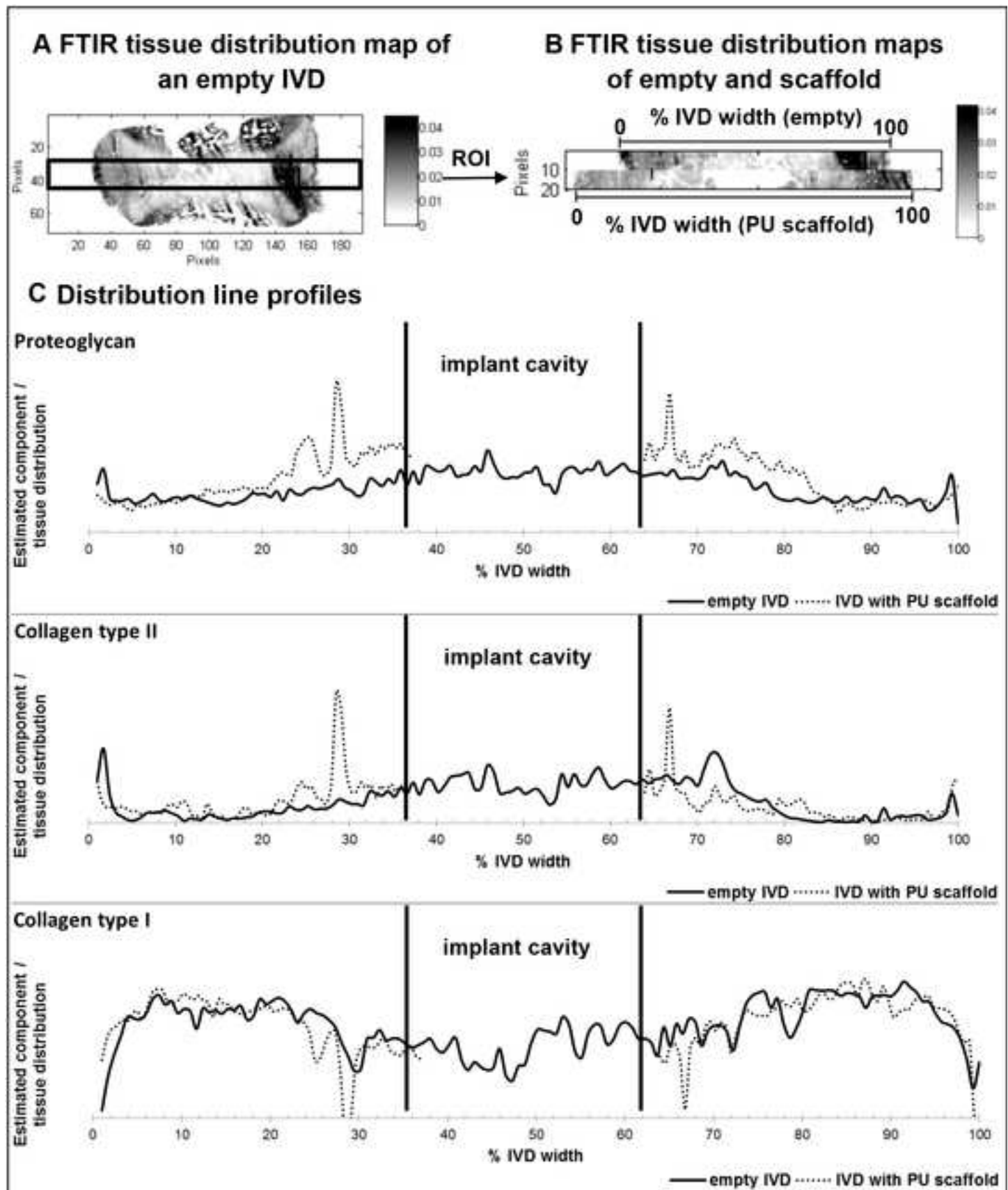


Figure Legends

Figure 1. (A) Flat discoid shaped PU scaffold before (front) and after (back) swelling at various sizes (from left to right 6, 9 and 14 mm). Each size has defined core content. (B) Scheme of PU scaffold assembly process: core disc is wrapped by two envelope discs, and heat sealed within a custom made sealing mold. (C) Non-invasive delivery system for PU scaffold: a demonstration of the scaffold insertion and swelling function after delivery and hydration.

Figure 2. SEM micrographs of electrospun PU scaffold envelope. Magnifications: left 2,000x; right 10,000x. Scale bar: left 50 μm , right 10 μm .

Figure 3. Swelling of PU scaffolds after 24 hours incubation in aqueous media tested at different core contents. Scaffold size: 14 mm in diameter.

Figure 4. Swelling kinetic of PU scaffolds at a diameter of 14 mm (A) and 6mm (B). For each scaffold diameter different amounts of core material were tested. Mean \pm SD, n=3.

Figure 5. (A-B) Cell number after culture in core and envelope conditioned media measured by WST-1 assay and normalized to positive control (cells cultured with DMEM/2.5% FBS). Mean \pm SD, n=3. (A) NPCs and MSCs cultured in conditioned medium of core for 24 hours or 72 hours. (B) NPCs and MSCs cultured in conditioned medium of envelope for 24 hours or 72 hours. (C) Representative SEM

images showing morphological structures of top surface and cross section of cell-seeded envelope constructs after 1 or 7 days of culture.

Figure 6. (A) Left: Macroscopic view of dry PU scaffold (diameter 6 mm) before implantation into partial nucleotomized IVD. Middle: Macroscopic sagittal view of partial nucleotomized IVD. Right: Macroscopic sagittal view of partial nucleotomized IVD with implanted PU scaffold after 24 hours of culture. PU scaffold swelled *in situ* and completely filled the nucleotomized region. (B) Dynamic compressive stiffness modulus of partial nucleotomized IVD before (defect) and after (refilled) refilling with PU scaffold, and after dynamic load and free swelling recovery (after dynamic load and recovery). Data were normalized to the stiffness modulus of respective intact IVD. (C) Disc height change of IVDs after dissection and free swelling culture overnight (intact), after partial nucleotomy (defect), after refilling with PU scaffold and free swelling culture overnight (refilled), after dynamic load (after dynamic load), and after free swelling recovery (after recovery). Data were normalized to initial disc height after dissection. (D and E) Representative stress/strain curves of IVDs from Empty and Scaffold groups at different time points. Mean \pm SD, n=6, * $p<0.05$, *** $p<0.001$ Empty *versus* Scaffold. Empty – partially nucleotomized IVDs, Scaffold – partially nucleotomized IVDs with implanted PU scaffold.

Figure 7. (A) Disc height change of partially nucleotomized IVDs without/with PU scaffold implantation under repetitive dynamic load. Mean \pm SD, n=6, * $p<0.05$, ** $p<0.01$, *** $p<0.001$ Empty *versus* Scaffold. (B-C) Relative mRNA expression of cells from remaining native NP and AF tissue in nucleotomized IVDs without/with PU scaffold implantation after 14 days of dynamic load. Data were normalized to the

gene expression level of disc tissue from respective bovine tail before starting organ culture on day 0. Mean + SD, n=8. Empty – partially nucleotomized IVDs, Scaffold – partially nucleotomized IVDs with implanted PU scaffold.

Figure 8. Representative Safranin O/Fast Green stained transverse sections of partially nucleotomized IVDs without/with PU scaffold implantation after 14 days of culture under dynamic load. (A, C) Overview of IVD without/with PU scaffold implantation, scale bar: 1000 μm . (B, D) Interface between remaining NP tissue and nucleotomized region without/with PU scaffold implantation, scale bar: 50 μm . Empty – partially nucleotomized IVDs, Scaffold – partially nucleotomized IVDs implanted with PU scaffold, s – PU scaffold, t – native disc NP tissue.

Figure 9. Representative FTIR tissue distribution map of a sagittal section of a partially nucleotomized IVD cultured for 14 days under dynamic load without PU scaffold (empty) (A). Image contrast for tissue distribution map is generated by integration of the 2nd derivative of the Amide III peak ($1186\text{-}1297\text{ cm}^{-1}$). The black square indicates a region of interest (ROI) which was used to investigate the matrix distribution of native disc tissue surrounding the implants cavity. FTIR tissue distribution maps of ROIs of an empty IVD (top) and an IVD implanted with the PU scaffold (bottom) cultured for 14 days under dynamic load (scale bar: white to black indicative of a low to high tissue content) (B). Estimated component per tissue distribution line profiles across the ROI normalised to 100 % IVD width of proteoglycan, collagen type II and collagen type I are shown for an empty IVD and a PU scaffold implanted IVD (C).